Preprints of the 19th World Congress
The International Federation of Automatic Control
Cape Town, South Africa. August 24-29, 2014

Extremum Seeking Control of an Optical Cavity ⋆

S. Z. Sayed Hassen, I. R. Petersen **

University of Mauritius, Réduit, Mauritius
(sayed.hassen@gmail.com)
** *University of New South Wales at ADFA, Australia*
(i.r.petersen@gmail.com)

Abstract: The frequency locking of optical cavities in the physics community has been traditionally performed using classical controllers. This approach works well as long as the system is not operating far from its linear region of operation. An optical cavity is however a highly nonlinear system and problems arise when it is affected by large disturbances. In this paper, we model the non-linearities arising in such an optical system and propose an extremum seeking controller to frequency lock the optical cavity. Simulation results are presented to validate the proposed scheme.

1. INTRODUCTION

The frequency locking problem arises in almost every quantum optics experiment. Optical cavities need to be stabilized before anything useful can be done (quantum experiment can be performed). The more stable the cavity is, the greater will be the sensitivity of the experiment. One of the most promising applications where frequency locking is of absolute importance is the interferometric gravitational wave detector (GWD) which requires a sensitivity of the order of 10^{-20}; see Aufmuth and Danzmann [2005]. It is believed that gravitational waves generated by extremely heavy celestial bodies can be strong enough to bend space and hence change the distance between two fixed points miles away by the minutest of amount. The role of the GWD is to detect this drift when it happens.

Traditionally, the Pound-Drever-Hall (PDH) (see Bachor and Ralph [2004]) approach is widely used in the physics community to achieve frequency locking in optical cavities. However, the approach has its limitations in that it works well as long as the system is operating close to resonance but it breaks down when the difference between the laser frequency and the resonant frequency of the cavity is too large. The difference between the laser frequency and the resonant frequency is regulated by controlling the position of a piezo-electric actuator which is glued to one of the cavity mirrors; see Figure 1. The cavity system comprises of a mechanical subsystem made up primarily of a piezo-electric actuator and an optical subsystem corresponding to the optical cavity. The two subsystems possess widely different time constants and this feature of the system allows the cavity system to be modeled as a linear dynamical system followed by a static nonlinearity. To circumvent this problem which arises when the difference between the laser frequency and the resonant frequency of the cavity gets too large, a time-varying Kalman filter which takes into account the inherent nonlinearities of the system was designed, successfully implemented and tested on a dSPACE system. Experimental results of this work are due to appear but simulation results of this work can be found in Sayed Hassen and Petersen [2010].

Optical cavities however have dynamics which can vary greatly with time. In particular, the nonlinearity present can change drastically with variations in temperature, humidity and to the slightest external mechanical disturbance. While the time-varying Kalman filtering approach in Sayed Hassen and Petersen [2010] works well as long as the nonlinearities are accurately modeled, the approach shows its limitations with changing parameters within the optical cavity. Moreover, the approach suffers from numerical problems as the order of the polynomial used to model the nonlinearities becomes too high. Also, the dynamical order of the linear part of the system has to be kept at a minimum to minimise computing time.

In this paper, we propose to use the extremum seeking control (ESC) approach which does not require explicit knowledge of the nonlinearity present in the system. Additionally, the only requirement for the approach to work is that an extremum exists. For the problem under consideration, the extremum occurs at the resonant frequency of the optical cavity. Given that the nonlinearity is ever changing, with this approach, the controller does not need to keep track or regulate about a given set point or value. Instead, the controller tracks a varying maximum of a performance output (in this case the transmittance output signal) and stabilizes the system at that extremum. The extremum seeking approach is in fact based on the premise that if the changes in the optimal reference occurs over a sufficiently long time interval, it is reasonable to assume that the system is static which in turn reduces the problem to that of an optimization problem; see Zhang and Ordóñez [2007]. The stability properties of the approach has been an issue of concern for some time and resulted in sparse applications of ESC. Local stability properties of a class of extremum seeking algorithms were proven for the first time in Krstić and Wang [2000] using averaging analysis and singular perturbation, resulting in a new impetus being

⋆ This work is supported by the Australian Research Council.

given to the approach and in a series of application papers; see, e.g., Tunay [2001]; Peterson and Stefanopoulou [2004]; Guay et al. [2004]; Banaszuk et al. [2004]; Li et al. [2004]. More recently, semi-global stability results were obtained by Moase and Manzie [2012].

The paper is divided as follows: in the next section, the operation of an optical cavity is briefly explained. The mathematical model of the optical cavity is derived in Sec. 3 and the repetitive nature of the cost function is also demonstrated. The problem is stated in Sec. 4 and the basis of operation of the extremum seeking scheme as well as the reasoning behind the choice of the ESC parameters is explained in Sec. 5. Simulation results are presented in Sec. 6 on a perturbed system under realistic conditions before we conclude.

2. OPTICAL CAVITY OPERATION

One of the most well known types of optical cavity is the Fabry-Perot cavity (see Bachor and Ralph [2004]) which is formed by two partially transmitting mirrors facing each other and which are spaced apart by large distances compared to the size of the mirrors. The mirrors are curved in such a way that the desired optical modes (transverse modes) set-up inside the cavity are well-defined with smooth and regular transverse patterns; see Siegman [1986]. The two waves traveling in the forward and reverse direction in a Fabry-Perot cavity set up an optical standing-wave which has a periodic spatial variation along the axis of the cavity with a period equal to one-half the optical wavelength. Depending on the length of the cavity, the plane waves propagating inside the cavity interact constructively resulting in stable optical modes and in a resonant mode, or destructively giving rise to unstable optical modes. The resonant frequency of an optical cavity depends upon its optical path length. The optical path length is usually modified by using a piezoelectric actuator attached to one of the mirrors of the cavity. In this way, the piezoelectric actuator adjusts the detuning variable Δ. Our aim is to frequency lock an optical cavity to a free running laser.

3. CAVITY MODEL

A schematic of the frequency stabilisation system is depicted in Figure 1. The laser mode b of frequency ω_0 is

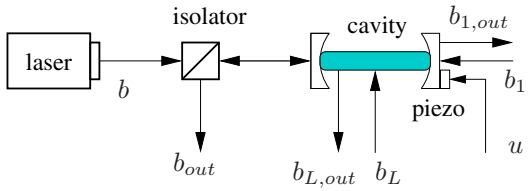

Fig. 1. Cavity locking feedback control loop.

modelled by a boson field $b = \beta + b_0$ where β is a real number (without loss of generality) and b_0 is a vacuum field, a standard quantum Gaussian white noise with unit variance; see Gardiner and Zoller [2000]. The cavity is also coupled to two other optical fields: a transmitted mode b_1, and a loss mode b_L.

The cavity can be described in the Heisenberg picture by the following quantum stochastic differential equations; e.g., see Bachor and Ralph [2004]; Gardiner and Zoller [2000]:

$$\dot{a} = -(\frac{\kappa}{2} - i\Delta)a - \sqrt{\kappa_0}(\beta + b_0) - \sqrt{\kappa_1}b_1 - \sqrt{\kappa_L}b_L; \quad (1)$$

$$b_{out} = \sqrt{\kappa_0}a + \beta + b_0; \quad (2)$$

$$b_{1,out} = \sqrt{\kappa_1}a + b_1. \quad (3)$$

Here, the annihilation operator for the cavity mode is denoted by a and the annihilation operator for the coherent input mode is denoted by $b = \beta + b_0$, both defined in an appropriate rotating reference frame (see Arnold [1989]), where b_0 is quantum noise. We write

$$\kappa = \kappa_0 + \kappa_1 + \kappa_L; \quad (4)$$

where κ represents the decay rate of the cavity and is usually measured in hertz(Hz). κ_0 quantifies the coupling strength of the field b_0 to the cavity. Similarly, κ_1 and κ_L quantify the strength of the couplings of the optical fields b_1 and b_L to the cavity respectively.

Δ denotes the frequency detuning between the laser frequency and the resonant frequency of the cavity. The objective of the frequency stabilisation scheme is to maintain $\Delta = 0$. The detuning is given by

$$\Delta = f_c - f_L = q\frac{c}{nL} - f_L, \quad (5)$$

where f_c is the resonant frequency of the cavity, f_L is the laser frequency, nL is the optical path length of the cavity, c is the speed of light in a vacuum and q is a large integer indicating that the q^{th} longitudinal cavity mode is being excited.

The cavity locking problem is formally a nonlinear control problem since the equations governing the cavity dynamics in (2) contain the nonlinear product term $\Delta\, a$.

3.1 Modelling

We continuously measure a quadrature of the laser field reflected by the cavity b_{out} using homodyne detection, producing a classical electrical signal y_1. The second measurement y_2 is obtained from $b_{1,out}$ and represents the transmitted light intensity (transmittance) from the cavity. The signal y_1 is measured using the standard homodyne detection method and includes a sensor noise v_1. Similarly, y_2 is measured using a photodiode and includes a sensor noise v_2. Figure 2 shows a block diagram of our system. The detuning Δ representing the difference between the cavity's resonant frequency from the laser frequency f_L is generated by the mechanical subsystem represented by the HV-amplifier and the piezoelectric actuator. The other noises that enter the optical cavity are the quantum noises.

We model the measurement of the X_ϕ quadrature of b_{out} via homodyne detection by changing the coupling operator for the laser mode to $\sqrt{\kappa_0}e^{-i\phi}a$, and measuring the real quadrature of the resulting field. The two output signals are respectively given by:

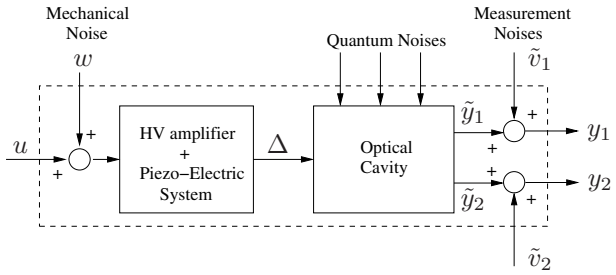

Fig. 2. Block diagram of the cavity system.

$$\begin{aligned}\tilde{y}_1 &= e^{-i\phi}b_{out} + e^{i\phi}b_{out}^\dagger \\ &= \sqrt{\kappa}_0(e^{-i\phi}a + e^{i\phi}a^\dagger) + 2\beta\cos\phi + q_0; \qquad (6)\\ \tilde{y}_2 &= b_{1,out}^\dagger b_{1,out} \\ &= \kappa_1 a^\dagger a + \sqrt{\kappa_1}(a^\dagger b_1 + b_1^\dagger a) + b_1^\dagger b_1; \qquad (7)\end{aligned}$$

where $q_0 = e^{-i\phi}b_0 + e^{i\phi}b_0^\dagger$ is standard Gaussian white noise. The cavity dynamics can then be expressed in state-space form in terms of the amplitude and phase quadrature variables as follows:

$$\begin{aligned}\begin{bmatrix}\dot{q}\\ \dot{p}\end{bmatrix} &= \begin{bmatrix}-\frac{\kappa}{2} & -\Delta\\ \Delta & -\frac{\kappa}{2}\end{bmatrix}\begin{bmatrix}q\\ p\end{bmatrix} - \sqrt{\kappa}_0\begin{bmatrix}\cos\phi & \sin\phi\\ -\sin\phi & \cos\phi\end{bmatrix}\begin{bmatrix}q_0\\ p_0\end{bmatrix}\\ &\quad - \sqrt{\kappa}_1\begin{bmatrix}1 & 0\\ 0 & 1\end{bmatrix}\begin{bmatrix}q_1\\ p_1\end{bmatrix} - \sqrt{\kappa}_L\begin{bmatrix}1 & 0\\ 0 & 1\end{bmatrix}\begin{bmatrix}q_L\\ p_L\end{bmatrix} - \begin{bmatrix}2\beta\sqrt{\kappa_0}\\ 0\end{bmatrix};\\ y_1 &= k_2\sqrt{\kappa_0}\,[\,\cos\phi\ \sin\phi\,]\begin{bmatrix}q\\ p\end{bmatrix} + k_2\,[\,1\ 0\,]\begin{bmatrix}q_0\\ p_0\end{bmatrix}\\ &\quad + 2k_2\beta\cos\phi + \tilde{v}_1;\\ y_2 &= \tilde{k}_2\left(\frac{\kappa_1}{4}(p^2+q^2) + \frac{\sqrt{\kappa_1}}{2}\,[\,q\ p\,]\begin{bmatrix}q_1\\ p_1\end{bmatrix}\right) + \tilde{v}_2.\end{aligned}$$

Here, y_1 is the output of the first sensor in which we have included the noise term $\tilde{v}_1$ and k_2 is the trans-impedance gain of the homodyne detector. Similarly, y_2 represents the measurement of the transmitted light intensity which includes the sensor noise $\tilde{v}_2$ and $\tilde{k}_2$ is the sensor gain of the associated photodiode.

3.2 Separation of time-scale approach to nonlinearity modeling

With the detuning variable Δ treated as an input signal in (8), this system is clearly nonlinear. The system (8) only behaves linearly when the variations of Δ about the linearised operating point are small. Under such circumstances, we can use linear control design techniques to control the system; see Sayed Hassen et al. [2009]. In the more general case, the detuning variable Δ is not necessarily small. In fact, it tends to be quite large and the linear control techniques discussed previously turns out to be inappropriate. In this section, we investigate the nonlinear behaviour of the measurement signals. Ignoring the noise terms q_0, p_0, q_1, p_1, q_L and p_L in (8), we can write

$$\dot{q} = -\frac{\kappa}{2}q - p\Delta - 2\sqrt{\kappa_0}\beta; \qquad (8)$$

$$\dot{p} = -\frac{\kappa}{2}p + q\Delta. \qquad (9)$$

In most problems of interest, the optical cavity has a very large value of κ, implying that it has a large bandwidth and is a very fast system compared to the mechanical subsystem. This feature allows for a decomposition of the system into stages that are dictated by a separation of time-scales. The end result is then a reduced model representing the dominant slowest phenomena together with a "boundary layer" model which evolves much faster and which represents deviations from the predicted slow behaviour. We use this approach to represent the optical cavity as a "boundary layer" model that acts like a static nonlinearity on Δ.

To determine the characteristics of this static nonlinearity, we set $\dot{q} = \dot{p} = 0$ in (8) and (9) and obtain

$$\begin{bmatrix}q\\ p\end{bmatrix} = \begin{bmatrix}-\frac{\kappa}{2} & -\Delta\\ \Delta & -\frac{\kappa}{2}\end{bmatrix}^{-1}\begin{bmatrix}2\sqrt{\kappa_0}\beta\\ 0\end{bmatrix} = -\frac{\begin{bmatrix}\kappa\beta\sqrt{\kappa_0}\\ 2\beta\sqrt{\kappa_0}\Delta\end{bmatrix}}{(\frac{\kappa}{2})^2 + \Delta^2}.$$

For the case when $\phi = \frac{\pi}{2}$ in (8), the two measurements available can then be written as:

$$\begin{aligned}y_1 &= k_2\sqrt{\kappa_0}p + 2k_2\beta\cos\phi + v_1\\ &= -\frac{2k_2\beta\kappa_0\Delta}{(\frac{\kappa}{2})^2 + \Delta^2} + v_1 = f_1(\Delta) + v_1; \qquad (10)\\ y_2 &= k_3(p^2+q^2) + v_2\\ &= \frac{k_3\beta^2\kappa_0}{(\frac{\kappa}{2})^2 + \Delta^2} + v_2 = f_2(\Delta) + v_2. \qquad (11)\end{aligned}$$

Here, we have combined all the noise terms together such that:

$$v_1 = \tilde{v}_1 + k_2\,q_0; v_2 = \tilde{v}_2 + \frac{\tilde{k}_2}{2}\sqrt{\kappa_1}\,[\,q\ p\,]\begin{bmatrix}q_1\\ p_1\end{bmatrix}; k_3 = \frac{1}{4}\tilde{k}_2\kappa_1.$$

Using typical experimental values for the parameters of the optical system (see Table 1), the plots shown in Figure 3 were generated to show the nonlinear effect of the detuning variable Δ on the measurement signals y_1 and y_2.

Simulation parameters	Value	Units
β	7×10^7	Hz
κ	1×10^5	Hz
κ_0	1×10^4	Hz
k_2	5×10^{-8}	V/Hz
k_3	8×10^{-9}	V

Table 1. Optical Cavity Model and Sensor Parameter Values.

It is clear from Figure 3 that maximum transmission occurs when the detuning variable Δ is zero. This occurs when the frequency of the laser's electromagnetic field is equal to the cavity's free spectral range (FSR) $= c/2L$.

4. PROBLEM STATEMENT

We consider the general problem of finding an extremum (minimum or maximum) of a nonlinear function. Let the system under consideration be described by the following nonlinear equations:

$$\dot{x} = f(x,u), \qquad (12)$$

$$y = J(x); \qquad (13)$$

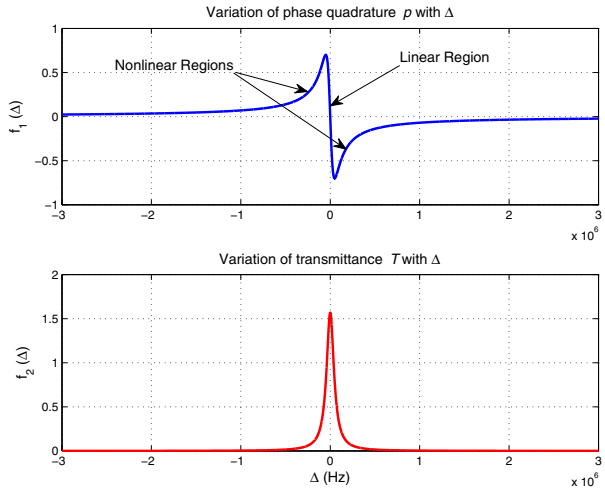

Fig. 3. Behaviour of the nonlinear measurement functions $f_1(\Delta)$ and $f_2(\Delta)$ with large variations in Δ.

where $x \in \mathbb{R}^n$ is the state, $u \in \mathbb{R}$ is the input, $y \in \mathbb{R}$ is the measured output as well as the performance output. $f : \mathbb{R}^n \times R \to \mathbb{R}^n$ and $J : \mathbb{R}^n \to \mathbb{R}$ are smooth functions and are in general unknown.

The aim is to design a controller to minimize (or maximize) the unknown function $J(x)$ or y and therefore minimize the performance output. The controller will use information from the performance output $J(x)$ and/or the gradient $\nabla J(x)$ to regulate the state x in finite time through the control input u, to eventually minimize the performance output. This controller exists if and only if (12) is controllable. The extremum seeking control problem is then posed as:

$$\min_{x \in \mathbb{R}^n} J(x), \text{ subject to } \dot{x} = f(x, u). \tag{14}$$

5. EXTREMUM SEEKING CONTROL

In Tan et al. [2010], ESC is defined as a "form of adaptive control where the steady-state input-output characteristic is optimized, without requiring any explicit knowledge about this input-output characteristic other than it exists and that it has an extremum." The approach has seen a resurgence in popularity recently as a result of a new stability analysis in Krstić and Wang [2000]. Numerous engineering problems which are inherently nonlinear and have either a local minima or maxima are potential candidates for the application of extremum seeking control.

For the optical cavity under consideration, we have shown that it can be conveniently modeled as a Hammerstein model, a model which is widely used to represent nonlinear dynamical systems. The system is broken up into 2 blocks, consisting of a linear dynamical block followed by a static nonlinearity. The continuous-time implementation of extremum seeking control applied to the optical cavity is depicted in Figure 4.

We will be using the measurement y_2 (transmittance) which is obtained from the static nonlinear block $f_2(z)$ and which is assumed to have a maximum $f_2^*(z)$. The proposed extremum seeking control scheme will tune the plant input u such that $f_2(z)$ is maximized. From Figure 4, the plant

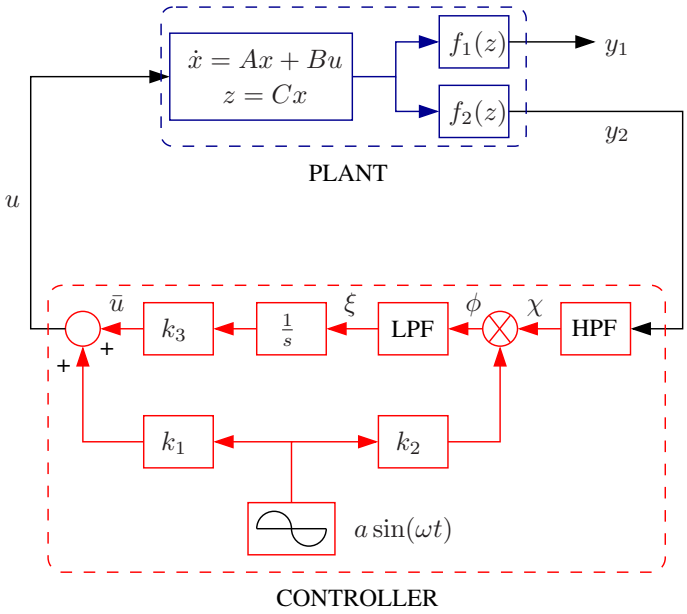

Fig. 4. Block diagram of the controlled system

input u is a superposition of a sinusoidal dither and a mean part $\bar{u}$. Moreover, by multiplying the plant output by the dither, we obtain a quantity, which in an averaged sense, is approximately proportional to the gradient of the input-output map $f_2'(\cdot)$. This information is then used by a gradient descent/ascent law to drive $\bar{u}$ towards the input that maximises $f(\cdot)$.

The purpose of the high pass filter is to isolate the variations of the measurement y_2 from the average value and to only preserve the perturbation. The resulting signal is then modulated by the same excitation (dither) signal $(a\sin(\omega t))$, which picks the component of the filtered signal with the same frequency ω as the probing signal. The resulting signal is then low pass filtered and is used as a measure of the gradient of the input-output map. An integral controller then determines the average component of the control signal that is to be fed to the plant to drive the estimated gradient to zero. The estimated gradient goes to zero when a maximum is reached in this case. If the high pass filter filter and the low pass filter are described by the first order transfer functions $\frac{\omega_h s}{\omega_h s+1}$ and $\frac{\omega_l}{s+\omega_l}$ respectively, then the extremum seeking control law in Figure 4 can be written as:

$$\dot{\chi} = -\frac{1}{\omega_h}\chi + \dot{y}_2; \tag{15}$$

$$\phi = k_2 \cdot a\sin(\omega t) \cdot \chi; \tag{16}$$

$$\dot{\xi} = -\xi + \omega_l \phi; \tag{17}$$

$$\dot{\bar{u}} = k_3 \cdot \xi; \tag{18}$$

$$u = \bar{u} + k_1 \cdot a\sin(\omega t). \tag{19}$$

An analysis of the stability of extremum seeking control was first rigorously performed in Krstić and Wang [2000] where local stability of a system with fairly general nonlinear dynamics was proven using averaging techniques and singular perturbation. In Tan et al. [2006], the results were extended to semi-global stability under stronger conditions. The approach however relied on having a slow dither

relative to the dynamics of the plant, which can result in very slow convergence. More recently, in Moase and Manzie [2012], this problem was investigated and semi-global stability results were obtained using a dither of arbitrary frequency on a class of SISO Hammerstein plant with fairly arbitrary nonlinearity.

5.1 Extremum seeking controller parameters

From Figure 4, it is clear that extremum seeking algorithms rely on a few design parameters. The performance of the scheme is linked with these parameters. Measures of performance could be (but not restricted to) the *speed of convergence*, the *domain of convergence* and the *accuracy*. Next, we explain the basis behind the choice of these parameters to meet these performance indicators.

Dither The "dither" or excitation signals employed in extremum seeking schemes in the literature generally tend to be sinusoidal. Other types of dither may work equally well or even better. It is argued in Tan et al. [2008] for example that square waves provide faster convergence than sinusoidal or triangular waves of the same amplitude and frequency. The reasoning behind this being simply that square waves yield larger normalized power.

Frequency A faster excitation frequency ω results in faster convergence. However, it should not be so fast to be completely attenuated by the dynamics of the plant, resulting in the extremum seeking scheme being driven by noise rather than the dither.

Gain The amplitude of the dither signal should be chosen so that it is small compared to $\bar{u}$ as it only ove the control signal. A small dither signal will ensur the cost function does not oscillate too much abo optimal value once that value has been reached.

Integrator gain The gain of the integrator k_3 am the average component of the control signal t applied to the plant.

High Pass Filter The high pass filter only allows tions beyond a certain frequency range in the sig to pass through.

Low Pass Filter The low pass filter only allows th frequencies (average values) to be integrated.

Ideally, one would expect the time-constant of the pass filter to be larger than that of the low pass filte the period of the dither to be in between the two v Moreover, the excitation signal should be small com to the integrator gain.

6. SIMULATION RESULTS

For the frequency locking cavity problem, we have chosen the parameters of the controller as shown in Table 2: The linear part of the plant is assumed to be a second order system with transfer function

$$P(s) = \frac{3.38 \times 10^7}{s^2 + 742.9s + 7.193 \times 10^7},$$

and its Bode plot is represented as shown in Figure 5.

The simulink block diagram used for simulation is shown in Figure 6. Both the phase quadrature y_1 and the transmittance y_2 as represented by (10) and (11) respectively

Parameters	Value
a	1×10^{-1}
ω	7×10^3
k_1	2×10^{-1}
k_2	5
k_3	6×10^3
ω_h	1×10^3
ω_l	1×10^2

Table 2. Extremum seeking controller parameter values.

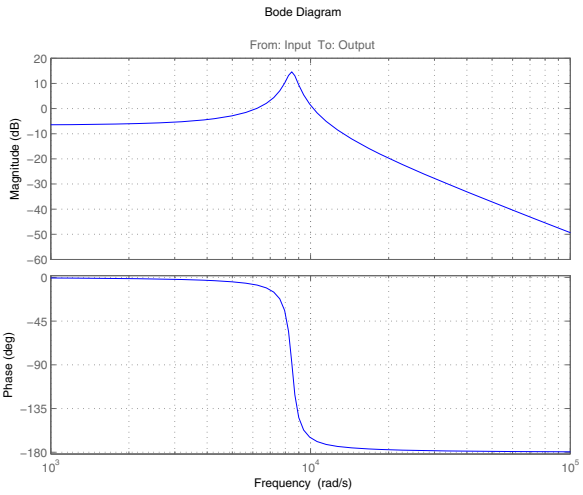

Fig. 5. Bode plot of the linear dynamics of the cavity

are measured, but only y_2 is used to control the system. White noises are also included in both measurements. We

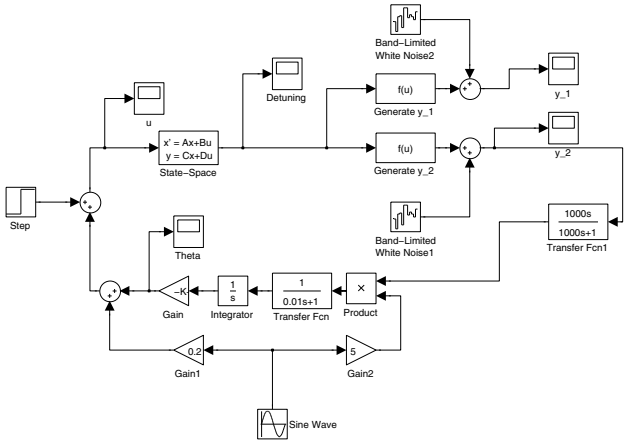

Fig. 6. Simulink block diagram

initiate the system away from lock at a detuning of 0.1 MHz and allow the extremum seeking controller to seek the extremum of y_2 and to lock onto the value. Then a step input of magnitude 5 volts is applied at the input of the plant at the time $t = 0.2$ second to simulate a disturbance. The response of the system is observed. Figure 7 shows the time response of the two measurement signals. It is clear that the extremum seeking control algorithm is successful in bringing the perturbed system back into lock after it has been pushed well outside its linear region of operation. The phase quadrature y_1 is brought back to zero while

the transmittance signal reaches its peak value about 0.5 seconds after the disturbance. It can also be noted that the algorithm used is quite aggressive in that it pushes the signal y_2 beyond its peak value before bringing it back. The corresponding detuning and control signal are also shown in Figure 8

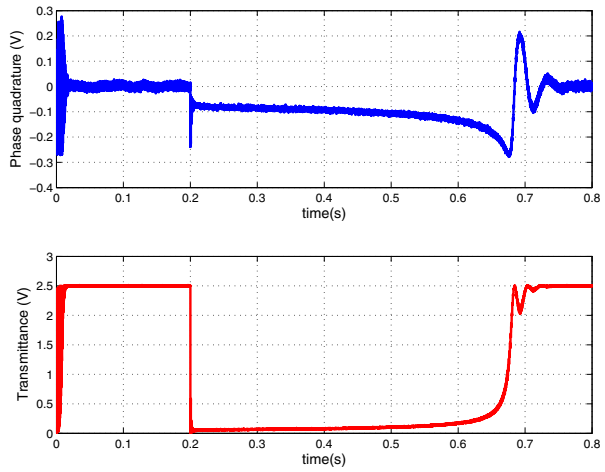

Fig. 7. Measurement signals y_1 and y_2

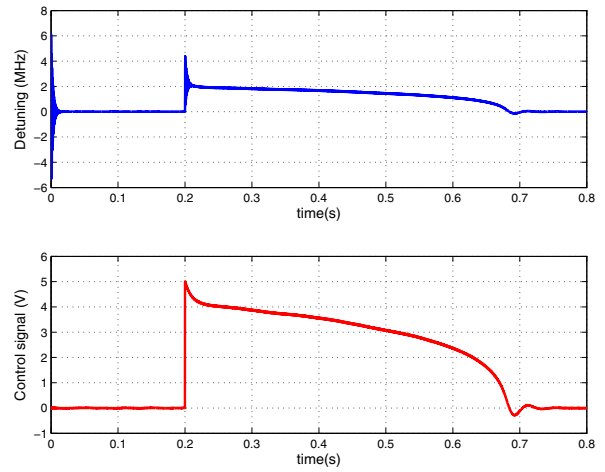

Fig. 8. Detuning Δ and control signal u

7. CONCLUSION AND FUTURE WORK

We have successfully applied the extremum seeking control approach to the frequency locking problem of a Fabry-Perot optical cavity. The nonlinearities arising in an optical cavity are derived using a singular perturbed approach and the overall system is represented as a Hammerstein model. The linear part of the model is reasonably approximated by a second-order system, with a resonant frequency at around 1300 Hz. The parameters of the extremum seeking controller are chosen on the basis of a series of performance requirements and indicators and the system was simulated with a relatively large disturbance introduced to push the cavity into its nonlinear region of operation. The controller was effective and prompt in bringing the system back into frequency lock. Work is in progress to implement the proposed control scheme on an experimental test bed and promising initial results have already been obtained.

REFERENCES

V. I. Arnold. *Mathematical Models of Classical Mechanics*. Graduate Texts in Mathematics. Springer, 1989.

P. Aufmuth and K. Danzmann. Gravitational wave detectors. *New Journal of Physics*, 7(202), Sept. 2005.

H. A. Bachor and T. C. Ralph. *A Guide to Experiments in Quantum Optics*. John Wiley, 2004.

A. Banaszuk, K. B. Ariyur, M. Krstić, and C. A. Jacobson. An adaptive algorithm for control of combustion instability and application to compressor instability control. *Automatica*, 40(11):1965–1972, 2004.

C. W. Gardiner and P. Zoller. *Quantum Noise*. Springer, Berlin, 2000.

M. Guay, D. Dochain, and M. Perrier. Adaptive extremum seeking control of continuous stirred tank bioreactors with unknown growth kinetics. *Automatica*, 40(5):881–888, 2004.

M. Krstić and H-H. Wang. Stability of extremum seeking feedback for general nonlinear dynamic systems. *Automatica*, 36(4):595–601, April 2000.

Y. Li, M. A. Rotea, G. T. C. Chiu, L. G. Mongeau, and I. S. Paek. Extremum seeking control of tunable thermoacoustic cooler. In *Proc. American Control Conf.*, pages 2033–2038, 2004.

W. H. Moase and C. Manzie. Semi-global stability analysis of observer-based extremum-seeking for hammerstein plants. *IEEE Trans. Autom. Control*, 57(7):1685–1695, July 2012.

K. S. Peterson and A. G. Stefanopoulou. Extremum seeking control for soft landing of an electromechanical valve actuator. *Automatica*, 40(6):1063–1069, 2004.

S. Z. Sayed Hassen and I. R. Petersen. A time-varying Kalman filter approach to integral LQG frequency locking of an optical cavity. In *Proc. American Control Conf.*, pages 2736–2741, Baltimore, MD, USA, July 2010.

S. Z. Sayed Hassen, M. Heurs, E. H. Huntington, I. R. Petersen, and M. R. James. Frequency Locking of an Optical Cavity using Linear-Quadratic Gaussian Integral Control. *J. Phys. B: At. Mol. Opt. Phys.*, 42 (17):175501, Sept. 2009.

A. E. Siegman. *Lasers*. University Science Books, 1986.

Y. Tan, D. Nešić, and I. Mareels. On non-local stability properties of extremum seeking control. *Automatica*, 42 (6):889–903, June 2006.

Y. Tan, D. Nešić, and I. Mareels. On the choice of dither in extremum seeking systems: A case study. *Automatica*, 44(5):1446–1450, May 2008.

Y. Tan, W. H. Moase, C. Manzie, D. Nešić, and I. M. Y. Mareels. Extremum seeking from 1922 to 2010. In *Proc. 29th Chinese Control Conference*, pages 14–26, Beijing, China, July 2010.

I. Tunay. Antiskid control for aircraft via extremum-seeking. In *Proc. American Control Conf.*, volume 2, pages 665–670, 2001.

C. Zhang and R. Ordóñez. Numerical optimization-based extremum seeking control with application to ABS design. *IEEE Trans. Autom. Control*, 52(3):454–467, Mar. 2007.